

Proceedings

# Low Impedance ALD HfO<sub>2</sub> Partially-Filled-Gap Flexural and Bulk MEMS Resonators Piezoresistively Detected for Distributed Mass Sensing<sup>†</sup>

Mariazel Maqueda Lopez, Emanuele Andrea Casu, Montserrat Fernandez-Bolanos and Adrian Mihai Ionescu \*

Nanoelectronic Devices Laboratory, EPFL, CH-1015 Lausanne, Switzerland; mariazel.maquedalopez@epfl.ch (M.M.L.); emanuele.casu@epfl.ch (E.A.C.); montserrat.fernandez-bolanos@epfl.ch (M.F.-B.)

\* Correspondence: adrian.ionescu@epfl.ch; Tel.: +41-21-693-3978

† Presented at the Eurosensors 2017 Conference, Paris, France, 3–6 September 2017.

Published: 9 August 2017

**Abstract:** This paper reports the design and characterization of partially-filled-gap capacitive MEMS resonators for distributed mass sensing applications. By filling the gap with HfO<sub>2</sub>, the coupling coefficient between electrode-resonator increases by ×6.67 times and the motional resistance decreases by ×12 times in comparison with its counterpart in air. An improvement by a factor of ×5.6 in the Signal-To-Noise Ratio (SNR) for DC bias up to ×2.8 lower is accomplished by performing a piezoresistive detection instead of capacitive detection. Quality factor (Q) of 11,350 and motional resistances (R<sub>m</sub>) of 926 Ω have been achieved for Parallel Beam Resonators (PBR) vibrating at 22.231 MHz. For the first time, ALD HfO<sub>2</sub> partially-filled-gap MEMS resonators are proven to achieve inertial distributed mass sensitivities of the order of 4.28 kHz/pg for beam-type and 1.8k Hz/pg for disk resonators.

**Keywords:** micromechanical resonator; MEMS resonator; MEMS; microsystems; microfabrication; silicon on insulator; quality factor; resonance frequency; mass sensing; mass sensor; Atomic Layer Deposition (ALD); high-k dielectric; hafnium oxide

---

## 1. Introduction

Capacitively transduced MEMS resonators have been proven to achieve resonance frequency times quality factor (fo×Q) products of the order of 10<sup>13</sup> [1], evidencing to be promising candidates to be used in communications [2] and environmental mass sensing applications [3]. Partially-filled-gap capacitive MEMS disks resonators were proposed in [4] to attain lower motional impedance, R<sub>m</sub>, better electromechanical coupling and more robustness against electrodes-resonator collapse. Similar devices have been proposed in [2] in order to overcome the power handling deficiencies of oscillators based on capacitively transduced disks.

Pursuant to investigating this approach for both flexural and bulk resonators targeted for mass sensing applications, several beam-type (clamped-clamped beam, CCB, double-ended tuning fork, DETF, and parallel beam PBR) and wine-glass disk (WGD) partially-filled gap resonators have been presented and characterized in the HF/VHF range in this work. Due to the gap reduction by means of the deposition of a high-k material such as hafnium oxide (HfO<sub>2</sub>, ε<sub>r</sub>~25), an increase in the capacitive coupling factor and a consequent lowering in the motional resistance have been obtained. In addition, an enhancement in the Q for the measured devices has been reported as a consequence of the gap filling fabrication process. Mass loading sensitivities have been evaluated for each

fabricated device, demonstrating the appeal of these devices for distributed mass sensing applications.

## 2. Design and Fabrication

The devices have been fabricated in a SOI wafer with a 1  $\mu\text{m}$  silicon thin layer n+ doped with phosphorous ( $\sim 10^{20} \text{ cm}^{-3}$ ) and a 1  $\mu\text{m}$  BOX layer. Gaps widths under 100 nm have been obtained by means of E-beam patterning and silicon DRIE process, (see Figure 1). The main dimensions and experimentally extracted parameters of the devices are shown in Table 1.

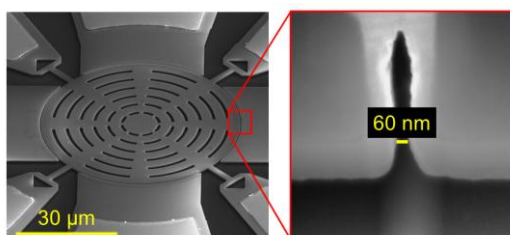


**Figure 1.** (a) SEM image of a released WGD with radius 30  $\mu\text{m}$  vibrating at 41.086 MHz; (b) FIB cross-section of the air-gap designed at 100 nm. The measured gap is narrower due to the material redeposition on the structure sidewalls during the FIB etching.

**Table 1.** Experimental parameters of the fabricated MEMS resonators after 5 nm of HfO<sub>2</sub> ALD.

| Device | R/lb <sup>1</sup> ( $\mu\text{m}$ ) | w <sub>b</sub> <sup>2</sup> ( $\mu\text{m}$ ) | g <sub>air,0</sub> <sup>3</sup> (nm) | f <sub>0</sub> (MHz) | Q <sup>4</sup> | R <sub>m</sub> ( $\Omega$ ) <sup>5</sup> | V <sub>DC</sub> (V) |
|--------|-------------------------------------|---|--------------------------------------|----------------------|----------------|--|---------------------|
| CCB    | 70                                  | 4   | 300                                  | 5.442                | 554            | 277.67 k                                 | 30                  |
| DETF   | 40                                  | 3   | 300                                  | 10.481               | 8190           | 28.16 k                                  | 50                  |
| PBR    | 151                                 | 5   | 100                                  | 22.231               | 11,350         | 926                                      | 70                  |
| WGD    | 30                                  | -   | 100                                  | 39.031               | 1065           | 40.35 k                                  | 50                  |

<sup>1</sup> radius/beam length; <sup>2</sup> beam width; <sup>3</sup> initial air-gap; <sup>4</sup> phase-slope approximation [5]. <sup>5</sup> R<sub>m</sub> = k<sub>eff</sub>/(( $\omega_0 \cdot Q \cdot \eta_{\text{eff}}$ )<sup>2</sup>) [6].

## 3. Results

Piezoresistive detection has been validated for WGD resonators (see Figure 1), evidencing to be the best detection method for capacitive resonators, showing an enhancement in the SNR level up to  $\times 5.6$  (Figure 2a) and anyways a distinguishable readability even for air-gaps as large as 300 nm (Figure 2b).

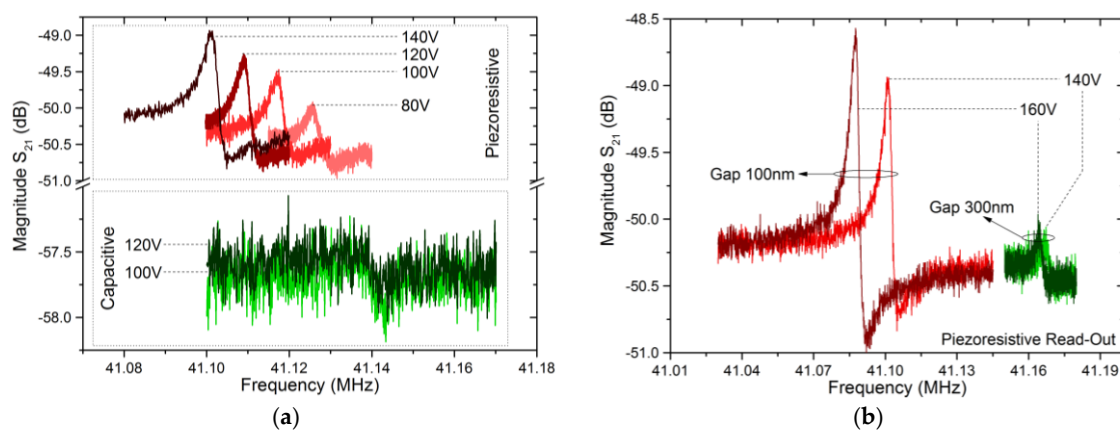


**Figure 2.** (a) S<sub>21</sub> response with capacitive and piezoresistive detection methods of a 100 nm air-gap WGD resonator; (b) S<sub>21</sub> response comparison of two WGD resonators with different nanometric air-gaps (100 nm and 300 nm) with piezoresistive detection. RF power -20 dBm.

Successive depositions of nanometric HfO<sub>2</sub> ALD layers have been performed in order to (a) partially-filling the transduction gaps with a high-k material to enhance capacitive transduction and lower motional resistance and (b) estimate and compare the distributed mass sensitivity for flexural and bulk resonators. Figure 3 shows the resulting slopes for the resonance frequency,  $f_0$ , downshift of a WGD after each HfO<sub>2</sub> deposition for both capacitive and piezoresistive read-outs, being the needed DC voltage up to  $\times 2.8$  lower for the latter.

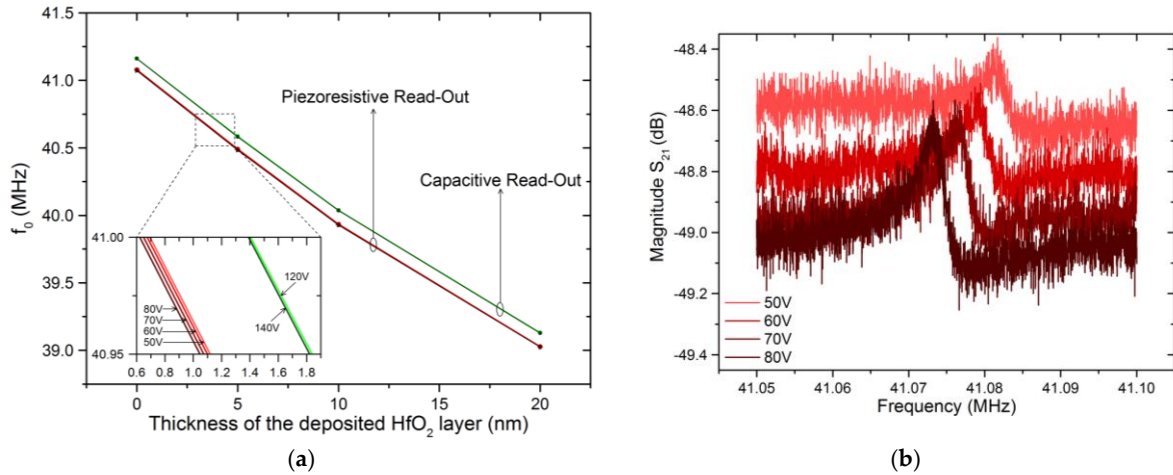


**Figure 3.** (a) Resonance frequency shifts for a WGD resonator after successive depositions of nanometric HfO<sub>2</sub> ALD layers; (b)  $S_{21}$  response of a WGD resonator for different nanometric air-gaps (piezoresistive detection) with no layer deposited. RF power  $-20$  dBm.

The successive HfO<sub>2</sub> depositions have caused a slight impoverishment of the probes-electrodes contact, worsening the transmission response level up to  $-20$  dB while keeping similar SNR levels (Figure 4a). A gain up to  $\times 7.3$  in the Q has been achieved for the partially-filled gaps DETF resonator after the first HfO<sub>2</sub> deposition (Figure 4b), overcoming the surface losses reported by [7].

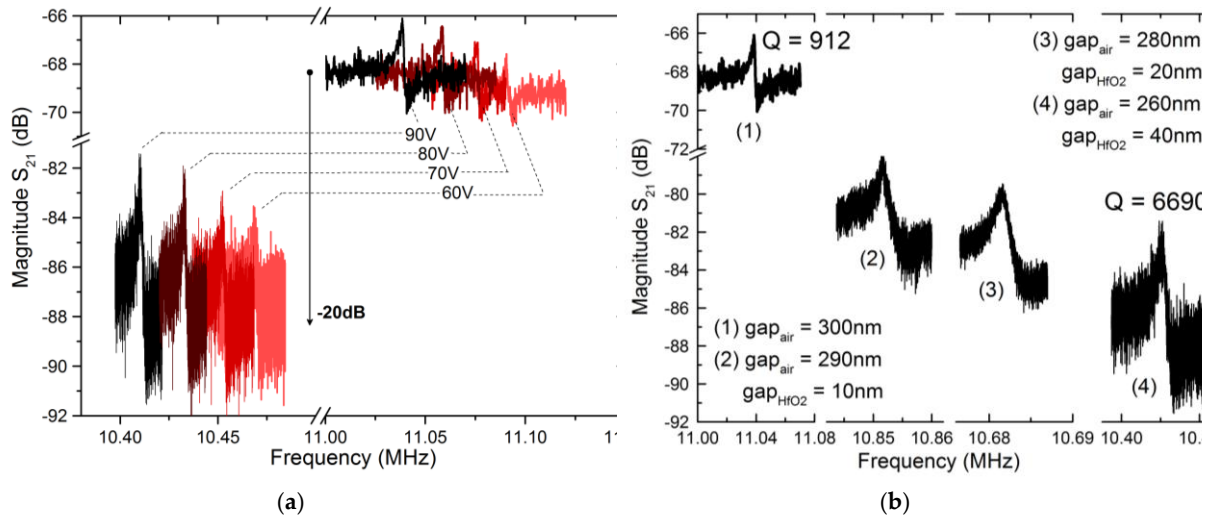


**Figure 4.** (a)  $S_{21}$  response of a DETF resonator for uncovered (right) and 20-nm HfO<sub>2</sub> ALD covered (left) cases; (b) Transmission signal level worsening after each HfO<sub>2</sub> ALD ( $V_{bias} = 90$  V).

Distributed mass sensitivity slopes have exhibited a linear frequency downshift with the added mass (Figure 5). Mass sensitivities of 4.28 kHz/pg for DETF and 1.8 kHz/pg for bulk WGD devices have been reported for the first time for partially-filled-gap resonators (Figure 6), values comparable to the ones presented in recent literature for MEMS resonators [3,8,9].

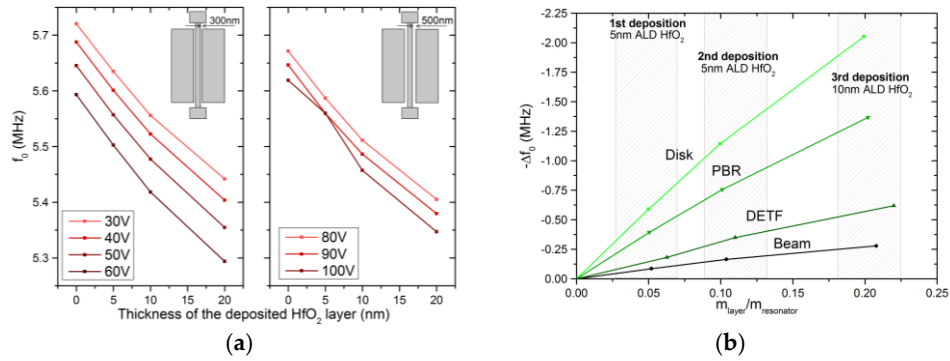


**Figure 5.** (a) Resonance frequency shifts of 300 nm-gap (left) and 500 nm-gap (right) CCB vibrating in the first flexural mode after  $\text{HfO}_2$  ALD depositions; (b) Comparison of the linear distributed mass sensitivity for bulk (WGD) and flexural (CCB, DETF and PBR) partially-filled  $\text{HfO}_2$  MEMS resonators.

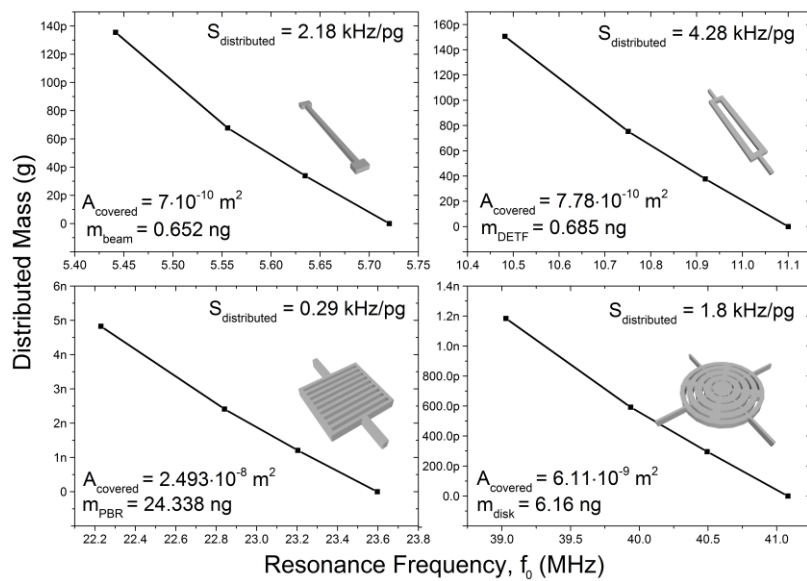


**Figure 6.** Experimental distributed mass sensitivity for the fabricated bulk (WGD) and flexural (CCB, DETF and PBR) partially-filled  $\text{HfO}_2$  MEMS resonators.

#### 4. Conclusions

In this work, bulk WGD and novel  $\text{HfO}_2$  partially-filled gap flexural resonators (CCB, DETF and PBR) have been presented. Their most relevant aspects have been analyzed: resonance frequency, quality factor, motional resistance and detection method. Maximum  $Q$  up to 11,350 and minimum  $R_m$  in the order of hundreds of ohms have been achieved (see Table 1). Distributed sensitivities of 4.28 kHz/pg for beam-type resonators and 1.8 kHz/pg for bulk disk resonators have been reported for the first time for partially-filled-gap resonators. A linear frequency downshift with the added mass has been detected despite the resonator stiffening after each  $\text{HfO}_2$  deposition, this aspect remains an open issue for further investigation.

**Acknowledgments:** The authors would like to thank the Swiss National Science Foundation (SNF) for the funds with which this work has been supported.

**Conflicts of Interest:** The authors declare no conflict of interest.

## References

1. Nguyen, C.T.-C. MEMS-based RF channel selection for true software-defined cognitive radio and low-power sensors communications. *IEEE Commun. Mag.* **2013**, *51*, 110–119.
2. Akgul, M.; Kim, B.; Lin, Y.; Li, W.; Huang, W.; Gurin, I.; Borna, A.; N, C. T.-C. Oscillator far-from-carrier phase noise reduction via nano-scale gap tuning of micromechanical resonators. In Proceedings of the TRANSDUCERS 2009–2009 International Solid-State Sensors, Actuators and Microsystems Conference, Denver, CO, USA, 21–25 June 2009; pp. 798–801.
3. Zarifi, M.H.; Daneshmand, M. Bulk disk resonators radial and wineglass mode resonance characterization for mass sensing applications. *Microsyst. Technol.* **2015**, *22*, 1013–1020.
4. Hung, L.; Jacobson, Z.A.; Ren, Z.; Javey, A.; and Nguyen, C.T.-C. Capacitive Transducer Strengthening Via ALD-Enabled Partial-Gap Filling. In Proceedings of the Solid-State Sensor, Actuator, and Microsystems Workshop, Hilton Head, SC, USA, 1–5, June 2004; pp. 208–211.
5. Frangiet, A. *Advances in Multiphysics Simulation and Experimental Testing of MEMS*; Imperial College Press: London, UK, 2008.
6. Tiffany, J.C.; Bhave, S.A. High-Q, low impedance polysilicon resonators with 10 nm air-gaps. In Proceedings of the 2010 IEEE 23rd International Conference on Micro Electro Mechanical Systems (MEMS), Wanchai, Hong Kong, China, 24–28 January 2010; pp. 695–698.
7. Lin, Y.; Li, S.; Xie, Y.; Ren, Z.; Nguyen, C.T.-C. Vibrating Micromechanical Resonators with Solid Dielectric Capacitive Transducer Gaps. In Proceedings of the 2005 IEEE International Frequency Control Symposium and Exposition, Vancouver, BC, Canada, 29–31 August 2005; pp. 128–134.
8. Hajjam, A.; Wilson, J.C.; Pourkamali, S. Individual air-borne particle mass measurement using high frequency micromechanical resonators. *IEEE Sens. J.* **2011**, *11*, 2883–2890.
9. Wasisto, H.S.; Merzsch, S.; Stranz, A.; Waag, A.; Uhde, E.; Salthammer, T.; Peiner, E. Femtogram aerosol nanoparticle mass sensing utilising vertical silicon nanowire resonators. *Micro Nano Lett.* **2013**, *8*, 554–558.



© 2017 by the authors. Licensee MDPI, Basel, Switzerland. This article is an open access article distributed under the terms and conditions of the Creative Commons Attribution (CC BY) license (<http://creativecommons.org/licenses/by/4.0/>).